Chapter 3

Polarized Light-Emission from Photonic Organic Light-Emitting Devices

Byoungchoo Park

Additional information is available at the end of the chapter

http://dx.doi.org/10.5772/54233

1. Introduction

Since the early pioneering work on efficient Organic Light-Emitting Devices (OLEDs) that was based on both small molecules and polymers, OLEDs have attracted a great deal of research interest due to their promising applications in full-color flat-panel displays and solid-state lighting [1-5]. Intensive research has been conducted into the development of OLEDs for realizing strong and efficient electroluminescent (EL) emission. To date, almost all previous work carried out on organic EL emission has involved unpolarized EL emission. Nevertheless, a number of researchers have reported the results of experiments in which linearly polarized EL emissions have been observed [6-17]. This particular avenue of research has been considered to be important because polarized EL emission from OLEDs is of potential use in a range of applications, not just those limited to high-contrast OLED displays, but also in efficient backlight sources in liquid crystal (LC) displays, optical data storage, optical communication, and stereoscopic 3D imaging systems [17]. In order to design and manufacture these novel light-emitting devices, a high degree of polarization ratio (*PR*) of emitting light is required, which has to be at least 30 ~ 40:1, between the brightness of two linearly polarized EL emissions that are parallel and perpendicular to the polarizing axis. Most cases of linearly polarized EL emission have been achieved through the use of uniaxially oriented materials, such as LC polymers or oligomers, incorporated within emissive layers. Methods that are commonly used for the uniaxial alignment of such layers include the Langmuir-Blodgett technique [6], rubbing/shearing of the film surface [7, 8], mechanical stretching of the film [9, 10], orientation on pre-aligned substrates [11, 12], precursor conversion on aligned substrates [13], epitaxial vapor deposition [14], and the friction-transfer process approach [15, 16]. Although there have been a number of such efforts to achieve linearly polarized EL emission, the polarization ratio and the device performance (in terms of brightness and efficiency) reported are still insufficient for most applications.

Here we introduce an approach different from the conventional methods using uniaxially oriented materials. As an alternative, for the purpose of improving device performance, we suggest a technique to control the polarization of light emitted from OLEDs that are achieved using an anisotropic photonic crystal (PC) film. It has been predicted that in anisotropic PCs, the photonic band structure splits with respect to the state of polarization of the interacting light, in contrast to the degenerated band structure of conventional isotropic PCs, in which a certain energy range of photons is forbidden, giving rise to a photonic band gap (PBG) [18-20]. Of these applications, the study of light emission at the PBG edge is particularly attractive, as a result of the fact that the group velocity of photons approaches zero and the density of mode changes dramatically at the PBG edge [21-24]. The combination of PCs with OLEDs has also been reported to achieve high out-coupling emission efficiency, as achieved in the micro-cavity OLEDs or multi-mode micro-cavity OLEDs [25-27]. Moreover, by employing the anisotropic photonic structure, one may also obtain the polarized emission of EL light.

In this chapter, we describe in brief a technique to control the polarization of EL light emitted from photonic OLEDs that make use of a *Giant Birefringent Optical* (GBO) [28] multilayer reflective polarizer [29-31] as the anisotropic PC film. When a large degree of birefringence is introduced into the in-plane refractive index between adjacent material layers of a multilayer photonic system, GBO effects begin to occur [28]. Pairs of groupings of adjacent layers (unit cells) can produce constructive interference effects when their thicknesses are scaled properly to the wavelength of interest. These interference effects in multilayered structures result in the development of alternating wavelength regions of high reflectivity (reflection bands) adjacent to wavelength regions of high transmission (pass bands) [28]. A significant optical feature of these multilayer interference stacks is the difference in the refractive index in the thickness direction (z axis) relative to the in-plane directions (x and y directions) of the film. By appropriate adjustment of the refractive indices of the adjacent layers, it is possible to construct a GBO multilayer reflecting polarizer using an interference stack that is composed of multiple layers of transparent polymeric materials [28]. The reflection band of the GBO polarizer exhibits a unique optical property, where the reflectivity of interference polarizers either remains constant or increases with increasing the angle of incidence. Furthermore, a graded unit cell thickness profile is normally used to create a wider reflective band that accommodates wavelengths from the blue through to the green and red color regions [28]. Such a multilayer polymer polarizer may routinely be used for optical applications that require high reflectivity and wavelength selectivity. As an example of this application, GBO multilayer polarizers have been used to create reflective polarizers that make LC displays brighter and easier to view. By using this property of the GBO polarizer, one might obtain highly linearly polarized EL light emission over a wide range of optical wavelengths. These anisotropic photonic effects of GBO cause the reflecting band structure to be polarized, and thus make it possible to show that such a combined OLED device can achieve polarized light-emission with high brightness and efficiency, resulting in a high *PR* value even for wideband EL emission from white light-emitting OLEDs (WOLEDs).

2. Polarized photonic OLEDs with GBO films

Three kinds of polarized photonic OLEDs are presented here to demonstrate the use of the GBO film in the highly polarized OLEDs, exhibiting high brightness and efficiency.

2.1. OLEDs on the GBO polarizer substrates

In this section, we describe the polarization of EL light emitted from OLEDs that use a flexible GBO multilayer reflecting polymer polarizer substrate, instead of the conventional isotropic glass substrate. By using such a substrate, we demonstrate the potential for highly polarized light emission from OLEDs. Luminous EL emissions are produced from the polarized photonic OLEDs, and the direction of polarization for the emitted EL light corresponds to the polarizing axis (transmission axis or passing axis) of the GBO reflecting polarizer. The estimated polarization ratio between the brightness of two linearly polarized EL emissions parallel and perpendicular to the polarizing axis can be achieved as high as 25 for the OLEDs on GBO substrates.

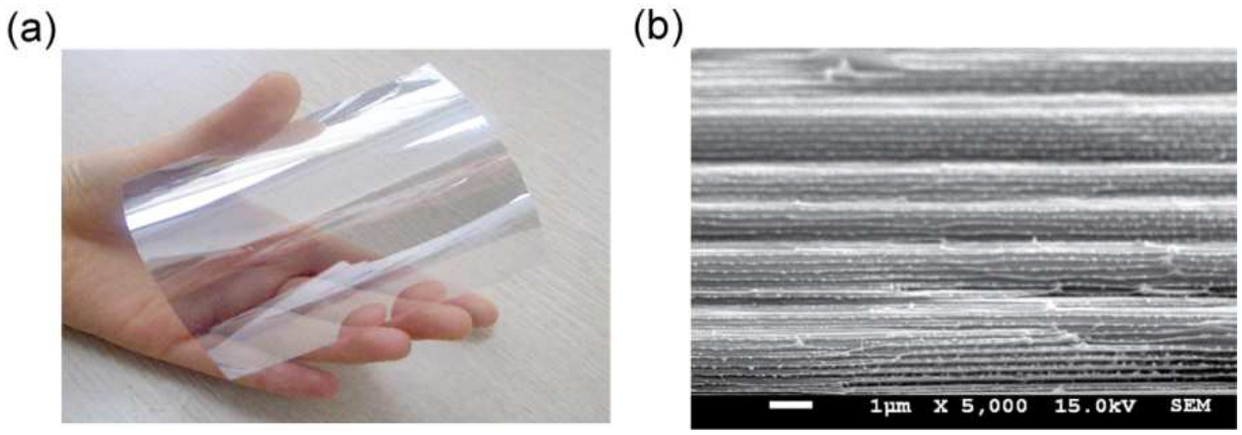

Figure 1. (a) Photograph showing the flexible transparent GBO reflecting polymer polarizer film and (b) SEM image of the cross-section of the studied GBO film.

2.1.1. Device fabrication and materials used

Sample OLEDs were prepared by placing an EL layer between an anode and a cathode on a flexible GBO reflecting polarizer film in the following sequence: GBO reflecting polarizer film substrate / thin semi-transparent Au anode / hole-injecting buffer layer / EL layer / electron-injecting layer / Al cathode. For the GBO reflecting polarizer film, a commercial multilayer reflecting polymer polarizer film (3M) has been used. The film is approximately 90 μm thick, and the wavelength of the reflection band is found to be in an approximate range of 400 ~ 800 nm. This film is normally used in an LC display backlight unit as a reflecting polarizer film. After routine cleaning of the GBO reflecting polarizer film using ultraviolet-ozone treatment, a flexible semi-transparent thin Au layer was deposited (90 nm, 40 ohm/square) by sputtering onto the GBO reflecting polarizer to form the anode. This Au anode is used in preference to the typical rigid indium-tin-oxide (ITO) anode in order to preserve the flexibility of the GBO polarizer substrate. The optical transmittance of the Au

electrode is about 60 % in the visible wavelength region. A solution of PEDOT:PSS (poly(3,4-ethylenedioxythiophene): poly(4-styrenesulphonate), Clevios PVP. Al 4083, H. C. Starck Inc.) is spin-coated onto the Au anode in order to produce the hole-injecting buffer layer. Subsequently, to form an EL layer, a blended solution is also spin-coated onto the PEDOT:PSS layer. This blended solution consists of a host polymer of poly(vinylcarbazole) (PVK), an electron-transporting 2-(4-biphenylyl)-5-(4-tert-butylphenyl)-1,3,4 oxadiazole (Butyl-PBD), a hole-transporting N,N'-diphenyl-N,N'-bis(3-methylphenyl)-1, 1'biphenyl-4,4'-diamine (TPD), and a phosphorescent guest dye of Tris(2-phenylpyridine) iridium (III) ($Ir(ppy)_3$), whose emission peak wavelength is ~510 nm with a full width at half maximum (FWHM) of ~85 nm [32]. A mixed solvent of 1,2-dichloroethane and chloroform (mixing weight ratio 3:1) is used for the solution. The thicknesses of the PEDOT:PSS and EL layers are adjusted to be about 40 nm and 80 nm, respectively. In order to form the electron-injecting layer, a ~1 nm thick Cs_2CO_3 interfacial layer is formed on the EL layer using thermal deposition (0.02 nm/s) at a base pressure of less than 2×10^{-6} Torr with a shadow-mask that had 3×3 mm^2 square apertures. Finally, a pure Al (~50 nm thick) cathode layer is deposited on the interfacial layer using thermal deposition under the same vacuum conditions. For comparison, we have also fabricated a reference device using a glass substrate in place of the GBO polarizer substrate. Apart from using different substrate materials, the reference devices are fabricated in exactly the same way as the sample OLED on the GBO polarizer substrate. Once the fabrication of OLEDs thus completed, the optical transmittance and reflectance spectra are measured using a Cary 1E (Varian) UV-vis spectrometer and a multichannel spectrometer (HR 4000CG-UV-NIR, Ocean Optics Inc., 0.25 nm resolution). A combination of a polarizer and an analyzer is also used to investigate the polarization of the light emitted from the sample device. A Chroma Meter CS-200 (Konica Minolta Sensing, INC.) and a source meter (Keithley 2400) have been used for measuring the EL characteristics.

2.1.2. Results and discussion

Figure 1(a) shows a photograph of the flexible GBO reflecting polarizer substrate used in this study. As shown in Fig. 1(a), the GBO substrate is easy to bend and quite transparent, in contrast to conventional linear dichroic polarizer film made from light-absorptive materials. Figure 1(b) shows a scanning electron microscopy (SEM) image of the cross-sectional structure of the GBO polarizer film. The SEM image shows clearly that the uniform layers of two alternating layered elements [a/b] are formed in multiple stacks with different refractive indices, (n_{ax}, n_{ay}, n_{az}) and (n_{bx}, n_{by}, n_{bz}). The optical anisotropy of the GBO polarizer may be seen by inspecting the polarized microphotograph of the GBO film between crossed polarizers at four angles of sample rotation of the GBO film substrate, as shown in Figure 2(a). This figure shows that the GBO film has a clear optical birefringence. We can define the orientation of the two optical axes, x and y, for the GBO film from the darkest views of the polarized microphotographs. The polarized transmittance spectra from the GBO polarizer film have then been observed for the two incident lights polarized linearly along the x and y axes, as shown in Figure 2(b). From this figure, it is clear that the nature of the reflection bands depends strongly on the polarization of the incident light, and the polarized

transmission spectra are thus quite different from each other. When measured in the *y* direction, the transmission spectrum shows a strong and broad reflection band, while in the *x* direction, there is no reflection band in the wide visible wavelength range (350 ~ 800 nm) that incorporates red, green, and blue light. This significant difference between the reflection bands clearly indicates that in a GBO reflecting polarizer film, the refractive indices of alternating layers are matched along both the *x*- and *z*- axes and mismatched along the *y*-axis. It is thus evident that the birefringence causes the reflecting band structure to be polarized and that the *x* and *y* axes represent the ordinary (*o*) and extraordinary (*e*) axes, respectively. Note that the *o* axis is consistent with the polarizing axis (or passing axis) and the *e* axis represents the blocking axis of the GBO reflecting polarizer. The average extinction ratio of the GBO reflecting polarizer used was estimated to be about 16:1 in the wavelength region between 470 and 700 nm.

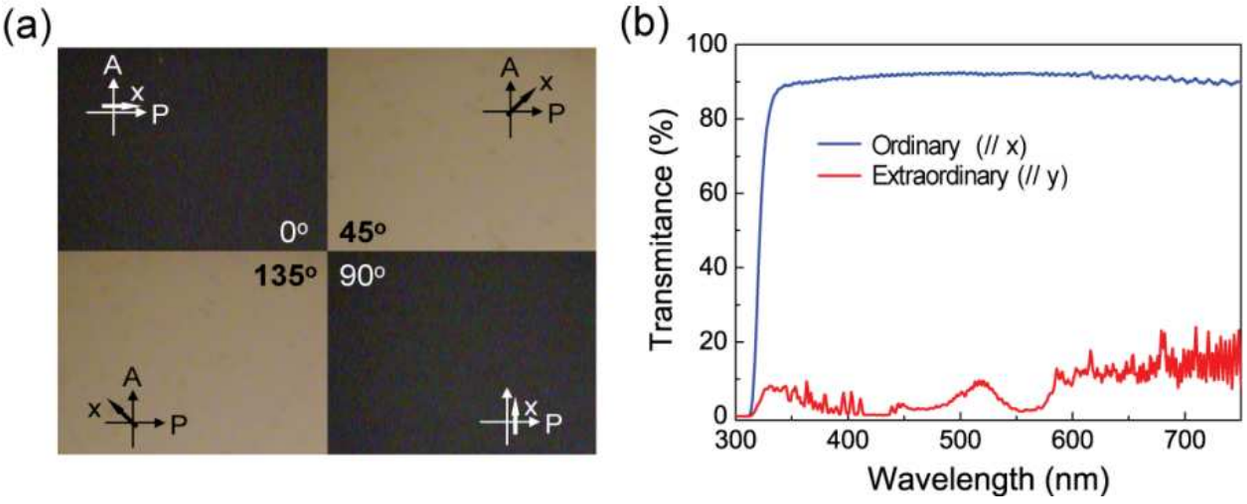

Figure 2. (a) Polarized microphotographs under crossed polarizers at four angles of sample rotation of the flexible GBO reflecting polymer polarizer film. (b) Polarized transmittance spectra for incident light polarized linearly along the *x* (ordinary) and *y* (extraordinary) axes.

On the design outlined above, we have prepared samples of OLEDs on the GBO reflecting polarizer substrate. In order to study the EL characteristics of the sample OLEDs, we have observed the current density-luminance-voltage (*J-L-V*) characteristics, as shown in Figure 3(a). It is clear from this figure that both the charge-injection and turn-on voltages are below 4.0 V, with sharp increases in the *J-V* and *L-V* curves. The EL brightness reaches ~4,500 cd/m^2 at 14.5 V. This performance of the sample OLED with respect to luminescence is nearly the same as that of the reference device using a conventional linear dichroic polarizer film, which shows ca. 5,000 cd/m^2 at 14.5 V. In contrast, as shown in Figure 3(b), the peak efficiencies (6.1 cd/A and 2.0 lm/W) of the sample OLED are much higher than those of the reference device (2.3 cd/A and 0.6 lm/W). The relatively high efficiencies of the sample device may be caused by the improved transition probability of exciton (singlet and triplet) relaxation with respect to the polarization along the transmission axis due to the reduced transition probability of exciton relaxation with respect to the polarization perpendicular to the transmission axis [20, 33].

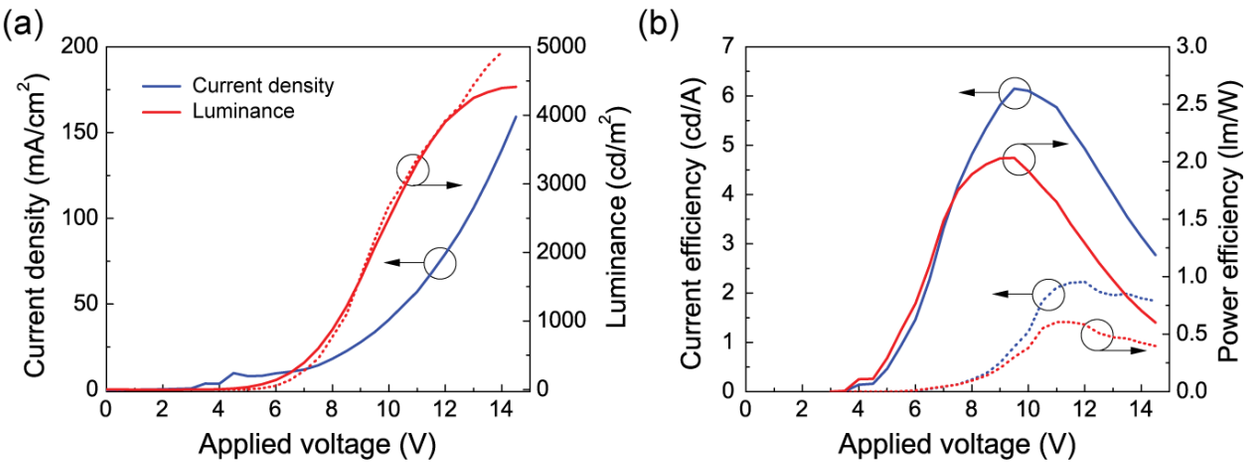

Figure 3. (a) Current density-voltage and luminance-voltage characteristics and (b) current efficiency-voltage and power efficiency-voltage characteristics of the sample OLED on the flexible GBO reflecting polarizer. The dotted curves show the characteristics of the reference device.

In order to interpret the observed EL characteristics of our sample device, we have also measured its polarization characteristics, as shown in Figure 4. Figure 4(a) shows the polarized EL emission spectra for the polarizations along the *o* ($EL_{||}$) and *e* ($EL\perp$) axes at normal incidence (0°). The curves represented by the dotted lines show the total spectra (*o* + *e*). It may be seen that the broad emission spectra are quite similar to that of the reference device, which coincides with the EL emission spectra of conventional OLED devices that have been reported elsewhere [32]. This figure also shows that polarized EL emission spectra strongly depend on the polarization state ($EL_{||}$ and $EL\perp$), and that the sample OLED exhibits highly polarized EL emission over the entire range of emission from 470 nm to 650 nm. The EL polarization ratio (*PR*) of the integrated intensities of the parallel ($EL_{||}$) and perpendicularly ($EL\perp$) polarized EL emission is approximately 25. This ratio is significantly higher than that of the reference device which shows a *PR* of 1 (unpolarized light emission). Here, the *PR* is deduced using the ratio of the intensities, which were measured with polarization parallel and perpendicular to the passing axis of the GBO film, respectively, *i.e.* $PR = EL_{||} / EL\perp$. These results show that this technique for assembling polarized OLEDs, which utilizes a GBO reflecting polarizer, is at least as good as the previous approach, which uses the alignment of uniaxially oriented polymers or oligomers.

Figure 4(b) shows the relative polarized *L-V* characteristics of the same OLED for the polarizations along the *o* and *e* axes. This figure also gives quantitative results for polarized light emissions that were observed along the *o* (||) and the *e* (⊥) axes. The highly polarized *L-V* characteristics give a high averaged *PR* value of 25 over the whole brightness range. (See Figure 5)

Next, as shown in Figure 6 are photographs of the operating polarized OLED sample (3 × 3 mm^2, 10 V) with the polarization along the *o* ($EL_{||}$, left) and *e* ($EL\perp$, right) axes of the flexible GBO reflecting polarizer substrate. It may be seen from the figure that under a rotatable linear dichroic polarizer (left), the OLED is relatively more luminous and highly polarized along the ordinary axis of the GBO polarizer substrate. From these results, we may conclude

that a flexible polarized OLED with a high polarization ratio can be fabricated successfully using the GBO reflecting polarizer substrate.

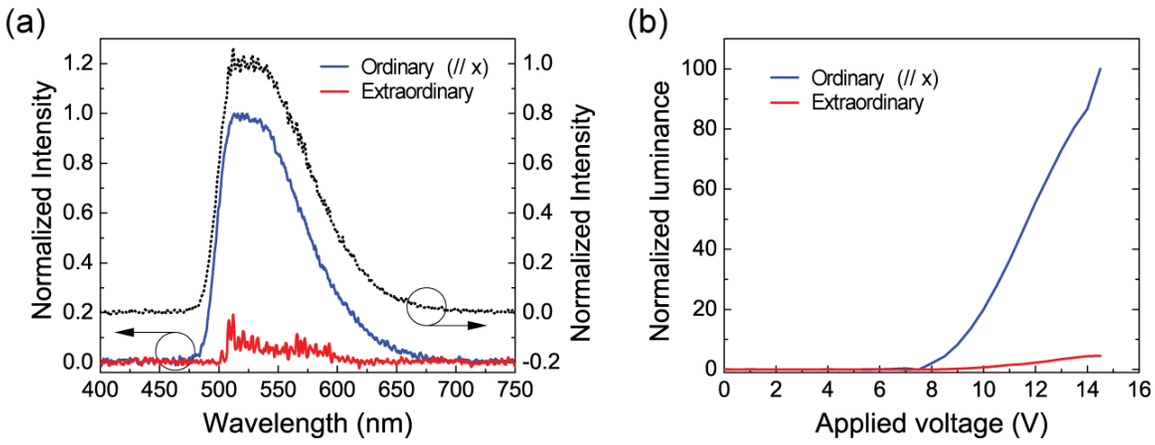

Figure 4. (a) Polarized EL emission spectra along the *o* ($EL_{||}$, blue solid curves) and *e* ($EL_{\perp}$, red solid curves) axes for the fabricated polarized OLED. The dotted curves show the total emission spectra (*o* + *e*). (b) The relative *L-V* characteristics for polarization along the *o* ($EL_{||}$) and *e* ($EL_{\perp}$) axes of EL emission.

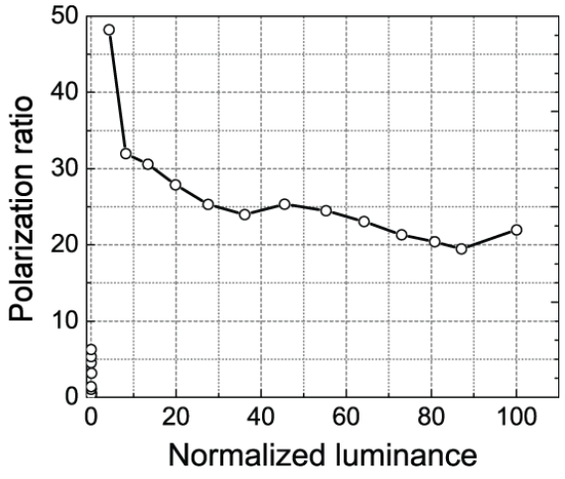

Figure 5. The polarization ratio characteristics obtained using the *L-V* characteristics shown in Fig. 4(b).

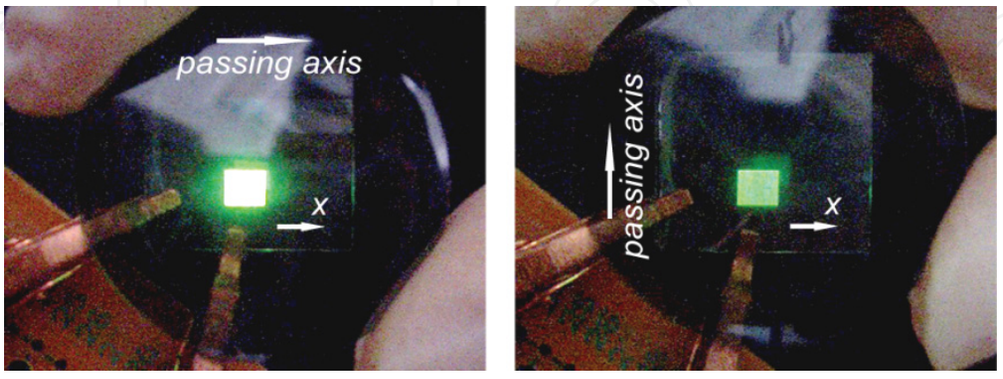

Figure 6. Photographs showing the operating polarized OLED sample (3 × 3 mm², 10 V) for the polarizations along the *o* ($EL_{||}$, left) and *e* ($EL_{\perp}$, right) axes of the flexible GBO reflecting polarizer substrate under a rotating linear dichroic polarizer film. The *passing axis* represents the polarizing axis (or transmission axis) of the linear dichroic polarizer.

2.1.3. Summary

In this section, we have presented the results of a flexible, polarized, and luminous OLED using a flexible GBO substrate. It is shown that EL brightnesses over 4,500 cd/m^2 can be produced using the sample OLED, with high peak efficiencies in excess of 6 cd/A and 2 lm/W. The polarization of the emitted EL lights from the sample OLED corresponds to the passing axis of the GBO polarizer substrate used. Furthermore, it is also shown that a high polarization ratio of up to 25 can possibly be achieved over the whole emission brightness range. These results show that use of GBO reflector enables the development of flexible OLEDs with highly polarized luminescence emissions.

2.2. OLEDs with a quarter waveplate film and a GBO polarizer film

We present here an alternative approach to achieving highly linearly polarized EL emission by resorting again on GBO films. We present a simple polarized OLED that can be driven by a 'photon recycling' concept, which is similar to that developed by Belayev et al [34]. We apply a quarter-wave retardation plate (QWP) film and a GBO reflective polarizer to a non-uniaxial OLED. The QWP film used in our study is a sheet of a birefringent (double refracting) material, which creates a quarter-wavelength (λ/4) phase shift and can change the polarization of the light from linear to circular and *vice versa*. Our combination of the QWP film with a GBO reflective polarizer has enabled us to achieve a high degree of linear polarization with high brightness and efficiency.

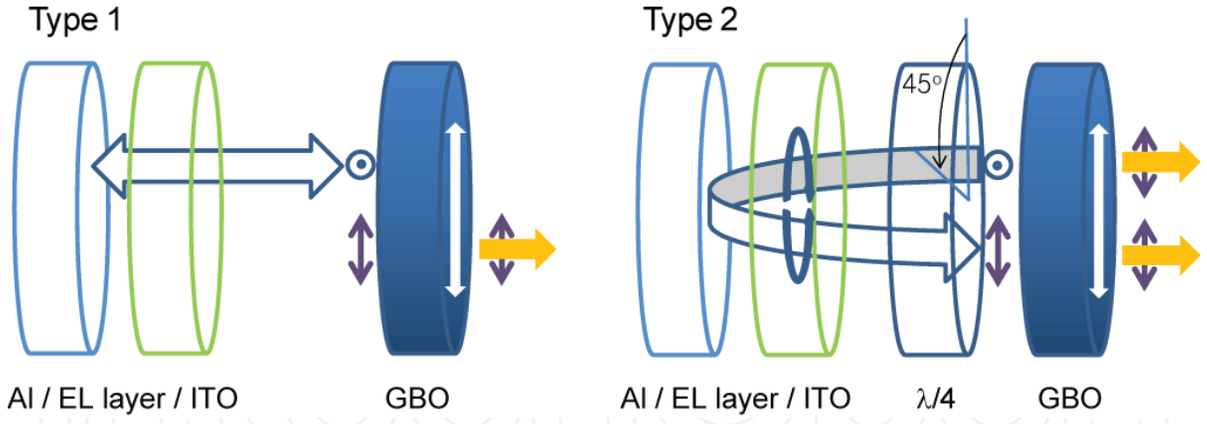

Figure 7. Schematic structures of polarized EL emitting OLEDs. Type 1: simple structure of a polarized OLED with a GBO reflective polarizer, Type 2: Combined structure of a polarized OLED with a QWP (λ/4 plate) film and a GBO reflective polarizer.

A schematic configuration of the device structure, designed to achieve highly linearly polarized EL emission is shown as Type 2 in Figure 7. For comparison, we have also shown the Type 1 device in Fig. 7, which is presented above in section 2.1. In this Type 2 device a QWP film and a GBO reflective polarizer are assembled on an OLED device, at an angle of 45° between the fast optic axis of the QWP film and the passing axis (↕) of the GBO polarizer, as shown in Fig. 7. Then the unpolarized EL light generated from the OLED gets linearly polarization state by QWP and GBO polarizer, as follows; The EL emission that is

polarized along the direction parallel to the passing axis (↕) of the GBO polarizer is transmitted through GBO, whereas the other EL polarized perpendicular (⊙) to the passing axis of the GBO polarizer is reflected back selectively as a result of the photonic band of the GBO polarizer. This reflected light changes its polarization to circular (*i.e.*, right-handed circularly polarized light) after its transmission through the QWP film. The sense of the rotation of this right-handed circularly polarized EL light is then changed by reflecting it from the surface of the metal cathode, *i.e.*, it now becomes left-handed circularly polarized light. Finally, by retransmitting it through the QWP film, the polarization of the light is again changed from left-handed circularly polarized to linearly polarized (↕). Now as the direction of polarization becomes parallel to the passing axis of the GBO it is transmitted through the GBO reflective polarizer. By this method, all generated EL light can be transmitted through the GBO reflective polarizer, has linear polarization (↕) along the passing axis of the GBO polarizer.

2.2.1. Device fabrication and materials used

The polarized OLEDs are prepared by placing an organic EL layer between an anode and a cathode on a glass substrate, together with a QWP film and a GBO reflective polarizer, in the following sequence: GBO reflective polarizer / QWP film / glass substrate / transparent ITO (80 nm, 30 Ω/square) anode / hole-injecting buffer layer / EL layer / electron-injecting layer / Al cathode (Type 2). A commercial QWP film (Edmund Sci.) approximately 110 μm thick and with a central operating wavelength of about 500 nm has been used. After a routine cleaning of the ITO substrate using wet (acetone and isopropyl alcohol) and dry (UV-ozone) processes, a solution of PEDOT:PSS is spin-coated onto the ITO anode in order to produce the hole-injecting buffer layer. Subsequently, in order to form an EL layer, a blended solution is also spin-coated onto the PEDOT:PSS layer. This blended solution consisted of a host PVK polymer, an electron-transporting butyl-PBD, a hole-transporting TPD and a phosphorescent guest dye of $Ir(ppy)_3$. A mixed solvent of 1,2-dichloroethane and chloroform (mixing weight ratio 3:1) was used for the solution. The thicknesses of the PEDOT:PSS and EL layers were adjusted to about 40 nm and 80 nm, respectively. In order to form the electron-injecting layer, a ~2 nm thick Cs_2CO_3 interfacial layer was formed on the EL layer using thermal deposition (0.02 nm/s) at a base pressure of less than 2×10^{-5} Torr. Finally, a pure Al (~50 nm thick) cathode layer was formed on the interfacial layer using thermal deposition by means of a shadow-mask that had square (3 mm × 3 mm) apertures under the same vacuum conditions. After the Al cathode had been formed, the QWP and the GBO films were attached sequentially to the ITO glass substrate using index-matching oil. In order to assess the effectiveness of our device, we also fabricated unpolarized conventional reference devices, using exactly the same method as for the polarized OLEDs but without the GBO and QWP films (1st reference device). For further comparison, 2nd reference device was also fabricated using only the GBO film Type 1, Fig. 7). It may be noted that in both type 1 and type 2 devices, the organic layer structure and organic materials used are identical, and thus, electrical characteristics such as the current density-voltage (*J-V*) curve are identical.

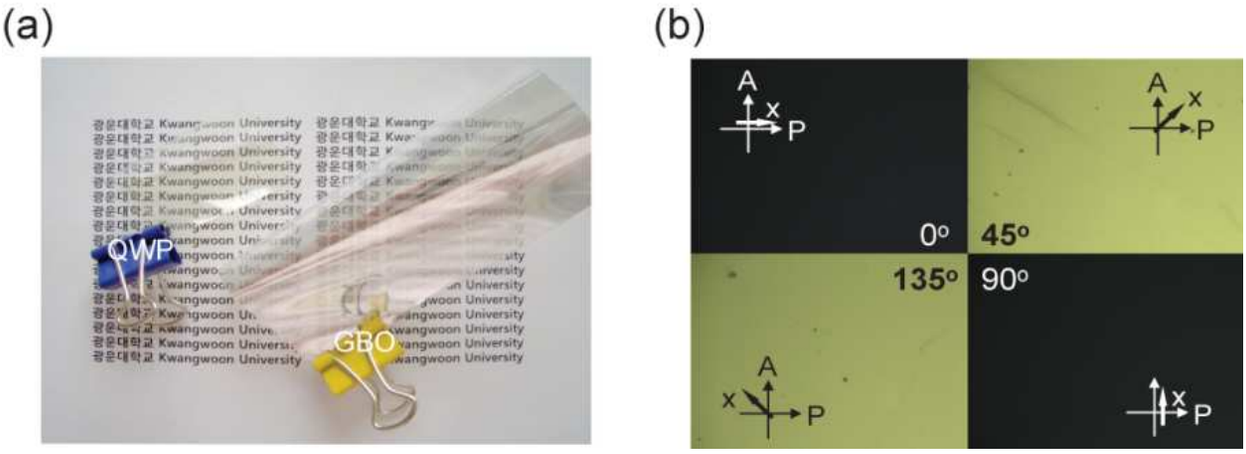

Figure 8. (a) Photographs of the transparent QWP film (left) and GBO reflective polarizer (right). (b) Polarized microphotographs at four angles of sample rotation of the QWP film.

2.2.2. Results and discussion

Figure 8(a) shows a photograph of the QWP film and the GBO reflective polarizer used in this study. As it can be seen the QWP film and GBO reflective polarizer are quite transparent. In Fig. 8(b), the optical anisotropy of the QWP film is shown in the polarized microphotograph obtained between crossed polarizers for four angles of rotation. Figure 8(b) shows that the QWP film has a clear optical birefringence. The two darker views of the polarized microphotographs enable us to obtain the orientation of the two optical axes for the QWP film.

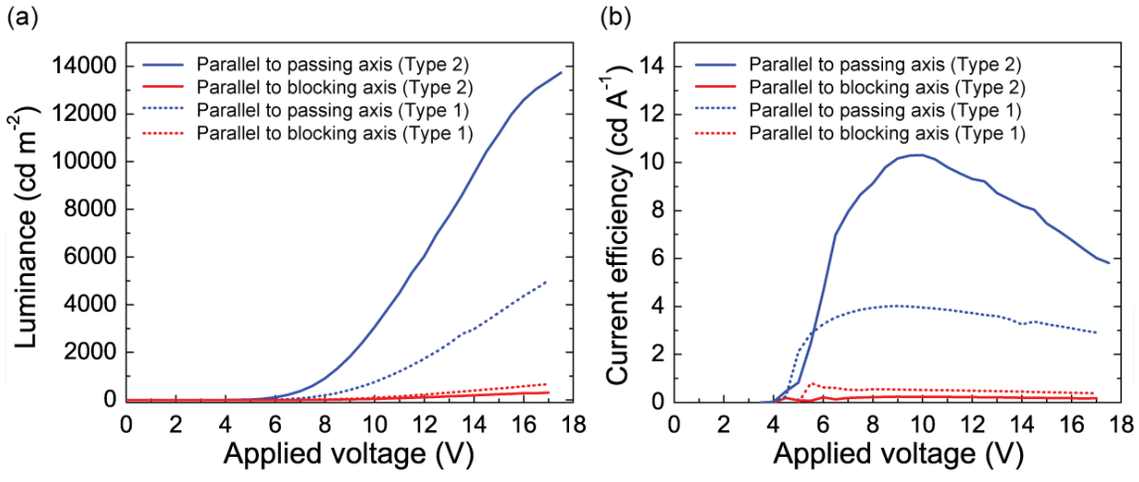

Figure 9. (a) Polarized *L-V* characteristics. ($EL_{||}$ blue and $EL_{\perp}$ red) (b) Current efficiency-voltage characteristics of the polarized OLEDs (solid curves). The dotted curves show the characteristics of the 2nd reference device.

The performance of the polarized OLEDs thus fabricated with the QWP film and the GBO reflective polarizer are presented here. Figure 9(a) shows the polarized *L-V* characteristics of the fabricated OLEDs for the polarizations along the passing ($EL_{||}$, blue curves) and the blocking ($EL_{\perp}$, red curves) axes. The figure indicates that the turn-on voltages are below 4.0

V (1 cd/m^2 in Fig. 9(a)) with sharp increases in the *L-V* curve for polarization parallel to the passing axis. The polarized EL brightness ($EL_{||}$) reaches ~13,400 cd/m^2 at 17.0 V. This performance with respect to luminescence approaches the luminescence of ca. 18,500 cd/m^2 at 17.0 V for the unpolarized 1st reference device, in which the QWP film and the GBO polarizer are omitted. The polarized *L-V* curves shown here also give quantitative results for the polarized light emissions observed along both the passing and blocking axes. As shown in Fig. 9(a), the highly polarized *L-V* characteristics for the polarized OLEDs give a high average *PR* of at least 40 over the whole voltage range (4.0 ~ 17 V). This ratio is significantly higher than that of the 1st and 2nd reference devices, which show *PR* of 1 (*i.e.*, unpolarized light) and 7.53, respectively. Fig. 9(a) also shows that the EL emission polarized along the passing axis reaches only ca. 5,000 cd/m^2 at 17.0 V for the 2nd reference OLED which only has the GBO polarizer. This performance of the 2nd reference OLED with respect to polarized luminescence along the passing axis of the GBO is only about the half. This relatively low brightness of the 2nd reference device is due to the absence of the 'photon recycling' effect mentioned above. It may also be seen that the EL brightness polarized along the blocking axis for the polarized OLEDs is further reduced compared with that of the 2nd reference OLEDs, as shown in Fig. 9(a). This is due to the reduced light intensity polarized along the blocking axis in the polarized device, following the change in the polarization to a direction parallel to the passing axis. Similarly, as shown in Figure 9(b), the peak efficiencies (10.3 cd/A and 3.63 lm/W) of the EL emission polarized along the passing axis for the polarized OLED are nearly double of that of the 2nd reference device (4.0 cd/A and 1.71 lm/W), while the efficiency of the EL emission polarized along the blocking axis for the polarized device is further reduced compared with that of the 2nd reference OLED.

We also measured the polarization characteristics and Fig. 10(a) shows the polarized EL emission spectra for polarizations along the passing ($EL_{||}$, blue solid curves) and blocking ($EL\perp$, red solid curves) axes at normal incidence, for an applied voltage of 10 V. It may be seen that the broad emission spectra are almost the same as those of the reference devices and conventional OLED devices reported elsewhere [32]. This figure also shows that the polarized EL emission spectrum depends very much on the polarization state, and that the polarized OLED shows highly polarized EL emission over the whole emission spectrum range. For the polarized device, *PR* of the integrated intensities of the $EL_{||}$ and $EL\perp$ lights is always greater than 40. It may therefore be concluded that our polarized OLEDs a QWP film and GBO reflective polarizer incorporated perform extremely well. Fig. 10(b) shows the *PR-L* characteristics of our polarized OLEDs. As shown in Fig. 10(b), in comparison with *PR* = 7.5 of the 2nd reference device our polarized device has a *PR* of over 40 in the whole brightness range.

The operation of the 2nd reference and polarized OLEDs (3 mm × 3 mm, 10 V) for polarizations along the passing and blocking axes of the GBO reflective polarizer is shown in Fig. 11. It may be seen from the figure that under a rotation of linear dichroic polarizer, right OLED is more luminous (left fig.) and more highly polarized along the passing axis of the GBO polarizer in comparison to the left 2nd reference device (right fig.). All these results

demonstrate a successful fabrication of a highly polarized OLED with a high *PR* (> 40), using a QWP film and a GBO reflective polarizer.

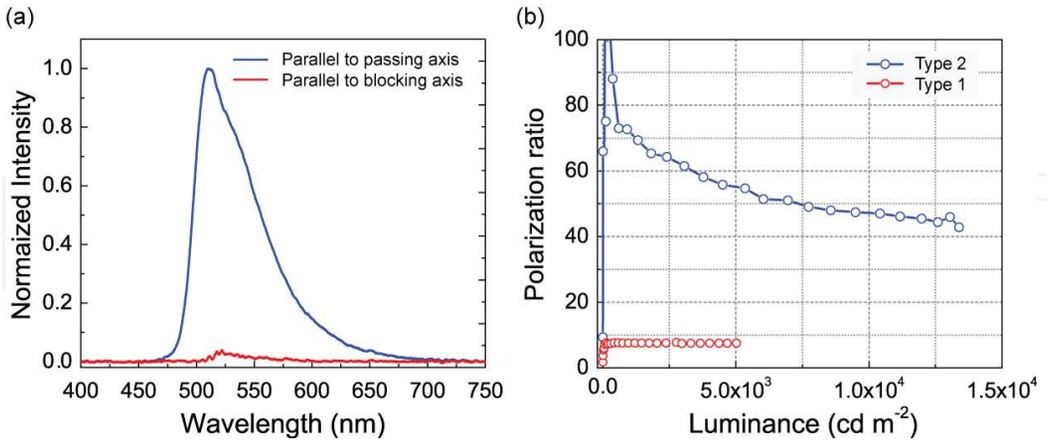

Figure 10. (a) Polarized EL emission spectra along the passing and blocking axes. (b) Polarization ratios of the polarized OLED (blue curve) against luminance. The points in red show the characteristics of the 2nd reference device.

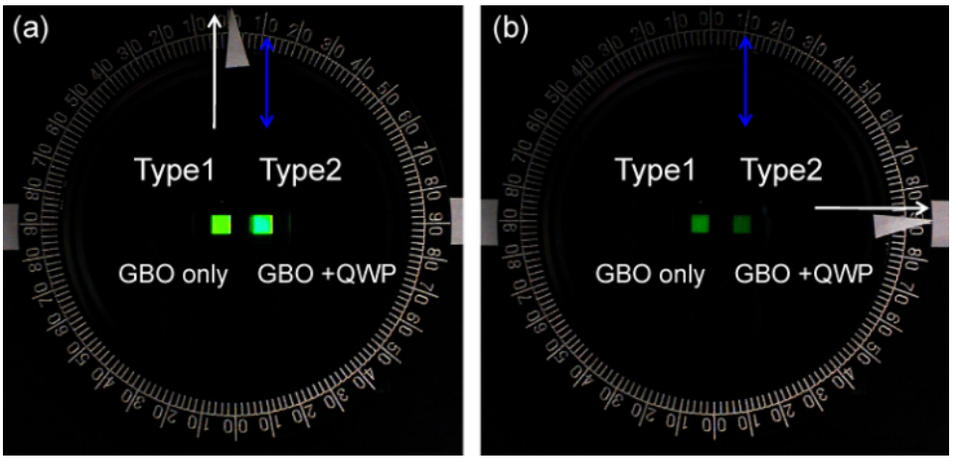

Figure 11. Photographs of the operating 2nd reference (left) and polarized (right) OLEDs for polarizations along the passing ($EL_{||}$) (a) and the blocking ($EL_{\perp}$) (b) axes of the GBO reflective polarizer under a rotating linear dichroic polarizer film. The white arrow represents the transmission axis of the linear dichroic polarizer and the blue arrow represents the transmission axis of the GBO polarizer.

2.2.3 Summary

In summary, we have described the fabrication and operation of a polarized and luminous OLED using the combination of a QWP retardation film and a GBO reflective polarizer. A peak polarized EL brightness of over ca. 13,000 cd/m² is produced from the polarized OLED, with high peak efficiencies in excess of 10 cd/A and 3.5 lm/W. The polarization direction of the EL light emitted from the polarized OLED corresponds to the passing axis of the GBO polarizer used. Furthermore, it has also been shown that a high polarization ratio greater than 40 is possible over the whole emission brightness range. These results show that using the QWP film and GBO reflective polarizer we can develop bright OLEDs with highly polarized luminescence emissions.

2.3. Polarized white OLEDs with achromatic QWP films on GBO substrates

Here we describe the third technique that can be used to achieve high linearly polarized white EL emission based on the 'photon recycling' concept [34] for a wide visible wavelength range including red, green, and blue light. We apply a GBO reflective polarizer to a WOLED with a broadband (achromatic) QWP film whose phase retardation is maintained at π/2 for a wide range of wavelengths, in contrast to the narrow band QWP used in section 2.2. The applied achromatic QWP film also creates a phase shift of a quarter of a wavelength (λ/4), and can change the polarization of the broad EL emission from linear to circular, and *vice versa*.

The configuration of the device is shown in Figure 12(a), which is nearly identical to Type 2 in presented in section 2.2 as shown in Figure 7. Here an achromatic QWP film and a GBO reflective polarizer are attached to a WOLED with an angle of 45° between the fast optic axis of the QWP film and the passing axis (↕) of the GBO polarizer. From the unpolarized EL light generated from the WOLED EL ($EL_{||}$) polarized along the direction parallel to the passing axis (↕) of the GBO polarizer is transmitted through the GBO polarizer. The EL ($EL_{\perp}$) polarized perpendicular (⊙) to the passing axis of the GBO polarizer is reflected selectively by the wide photonic band of the GBO polarizer. The polarization of this reflected light is changed to right-handed circular (*R*) after its transmission through the achromatic QWP film. The sense of rotation of this circularly polarized EL light is then reversed to left-handed circular (*L*) by reflecting it from the surface of the metal cathode. Then by retransmission of this light through the achromatic QWP film changes its polarization again from circularly to linearly polarized (↕), which can be transmitted through the GBO reflective polarizer. This method allows nearly all the generated white EL light to be transmitted through the GBO reflective polarizer with a direction of linear polarization (↕) parallel to the passing axis of the GBO polarizer.

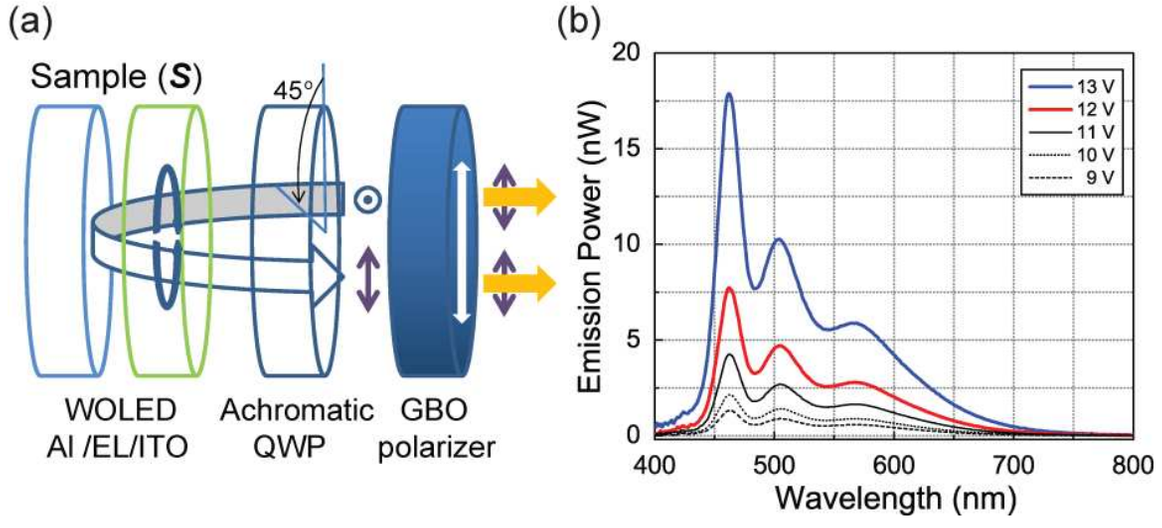

Figure 12. (a) Polarized WOLED (*S*) combined with an achromatic QWP (λ/4 plate) film and a GBO reflective polarizer: Type 2 and (b) Unpolarized EL spectra of the WOLED used for the polarized WOLEDs.

2.3.1. Device fabrication and materials used

The polarized WOLEDs were prepared by fabricating organic layers between an anode and a cathode on a glass substrate, together with a commercially available achromatic QWP film and a GBO reflective polarizer. The QWP film was approximately 110 μm thick, and the range of its operating wavelengths were approximately 420 ~ 650 nm. After routine cleaning of the ITO (150 nm, 10 Ω/square) substrate using both wet (acetone and isopropyl alcohol) and dry (O_2 plasma) processes, the organic layers were deposited on the ITO anode to form the structure of the tandem hybrid WOLED: ITO anode / short reduction layer (5 nm) / hole injection layer 1 (10 nm) / hole injection layer 2 (25 nm) / fluorescent blue-light emitting material layer (10 nm) / 8-hydroxy-quinolinato lithium (Liq)-doped electron injection layer (20 nm) / Li doped electron injection layer (20 nm) / hole injection layer 3 (10 nm) / hole transporting layer (55 nm) / phosphorescent green- and red-light emitting material layer (25 nm) / hole blocking layer (10 nm) / Liq doped electron injection layer (30 nm) / Al cathode. This is similar to the structure reported in reference [35]. The organic layers and Al cathode (150 nm) were deposited consecutively by thermal evaporation in a chamber with a base pressure of less than 1×10^{-6} Torr by means of a shadow-mask with square (1 mm × 1 mm) apertures. When the cathode was ready, the achromatic QWP and the GBO films were combined sequentially to the fabricated WOLEDs (device *S*). For comparison, we also fabricated reference devices, using exactly the same method as for the WOLEDs, but with only the GBO film (reference device *R*). The structure of the organic layer and the organic materials used were identical for each of the devices described herein. Figure 12(b) shows the white-light EL spectra (unpolarized) observed for the fabricated WOLED, in which three balanced emission peaks may be seen at 463 (blue), 503 (green), and 563 (red) nm. The spectral shape of the EL spectrum emitted from the device did not change significantly with applied voltage, and the color coordinates varied by less than 10% for the applied voltages between 7 ~ 14 V.

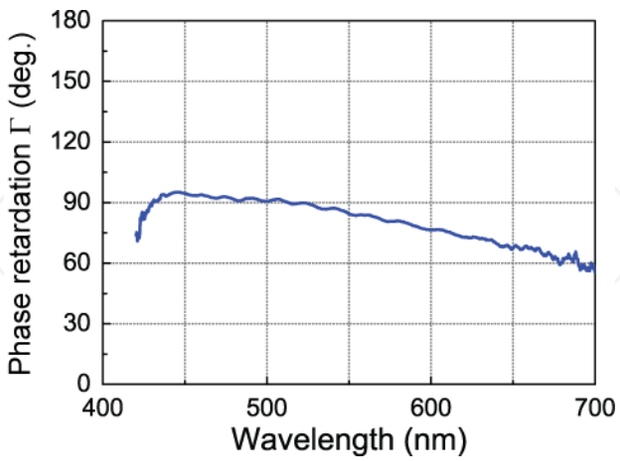

Figure 13. Phase retardation (Γ) of the broadband achromatic QWP film used in this study.

2.3.2. Results and discussion

The phase retardation (Γ) of the achromatic QWP film used in this study is measured by observing the transmission T ($T = 1/2 \sin^2(2\phi) \sin^2(\Gamma/2)$) through the QWP film placed

between crossed polarizers. Here, ϕ represents the angle between a fast axis of the achromatic QWP film and a transmitting axis of the polarizer. The measured results are shown in Figure 13. This figure shows clearly that the phase retardation of the achromatic QWP film is about $\pi/2$. Although the retardation decreases slightly as the wavelength increases, the QWP film has a nearly uniform phase retardation of a quarter of a wavelength ($\lambda/4$) in a wide visible range of wavelengths (420 ~ 650 nm) that includes blue, green, and red light.

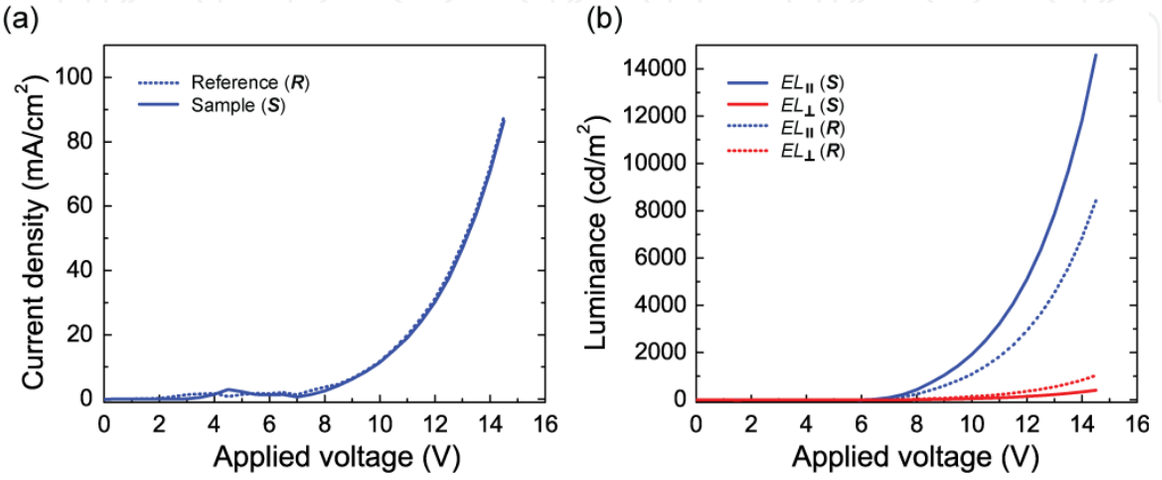

Figure 14. (a) *J-V* and (b) polarized *L-V* characteristics of Reference (*R*, dotted curves) and Sample (*S*, solid curves) WOLEDs.

Figure 14(a) shows the *J-V* curves of the fabricated WOLED devices *S* and *R*. For all the WOLEDs described herein, the organic layers used are the same, and the electrical characteristics (such as *J-V* curves) are therefore found to be identical for each device as shown in Fig. 14 (a). Figure 14(b) shows the *L-V* characteristics of the WOLEDs for $EL_{||}$ (blue curves) and $EL_{\perp}$ (red curves). Figure 14(b) shows clearly that the devices operate at relatively low turn-on voltages (~ 6 V) and have bright EL emissions, which indicate the efficient emission of white EL from the WOLEDs. It is noteworthy that even without full operational optimization of the polarized WOLED, its performance shows its potential attractiveness. In particular, the WOLED with both the GBO and achromatic QWP films (device *S*) exhibits excellent performance, in which operating voltages of about 7.0 and 8.7 V are required to obtain brightnesses ($EL_{||}$) of 100 cd/m² and 1,000 cd/m², respectively, with a peak luminescence of ca. 14,600 cd/m² at 14.5 V. It may be seen that the peak luminance ($EL_{||}$) of the device *S* under test is much higher than that of a previously reported polarized WOLED (ca. 850 cd/m² in Ref. 8) that used a uniaxially oriented polymeric material as an EL layer. Figure 14(b) also shows that the $EL_{||}$ reaches only ca. 8,400 cd/m² at 14.5 V for device *R*, whose performance with respect to $EL_{||}$ is only about half as good as that of device *S*.

In Fig. 15 (a), we have shown the current efficiencies of S and R WOLEDs. For the $EL_{||}$ of device *S*, a current efficiency (η_C) of 16.5 cd/A is obtained at 100 cd/m² (7.0 V), reaching η_C = 18.3 cd/A at 1,000 cd/m² (8.7 V) and η_C = 16.5 cd/A at 14,600 cd/m² (14.5 V). We have also determined the power efficiency η_P for the $EL_{||}$ of device *S*, which increases and reaches a maximum of 7.4 lm/W before slowly decreasing, with increasing bias voltage as shown in

Figure 15(b). These results indicate that the peak efficiencies (18.3 cd/A and 7.41 lm/W) for the $EL_{||}$ of device *S* are nearly double those of device *R* (9.63 cd/A and 3.71 lm/W). These relatively high brightness and efficiency values of the $EL_{||}$ of device *S* are achieved by the 'photon recycling' effect. It is noted that the brightness and efficiency of $EL\perp$ for device *S* are further reduced compared with those of device *R*, as shown in Figures 14 and 15. This is due to the reduced $EL\perp$ in device *S* that occurred after the change in polarization to the direction parallel to the passing axis.

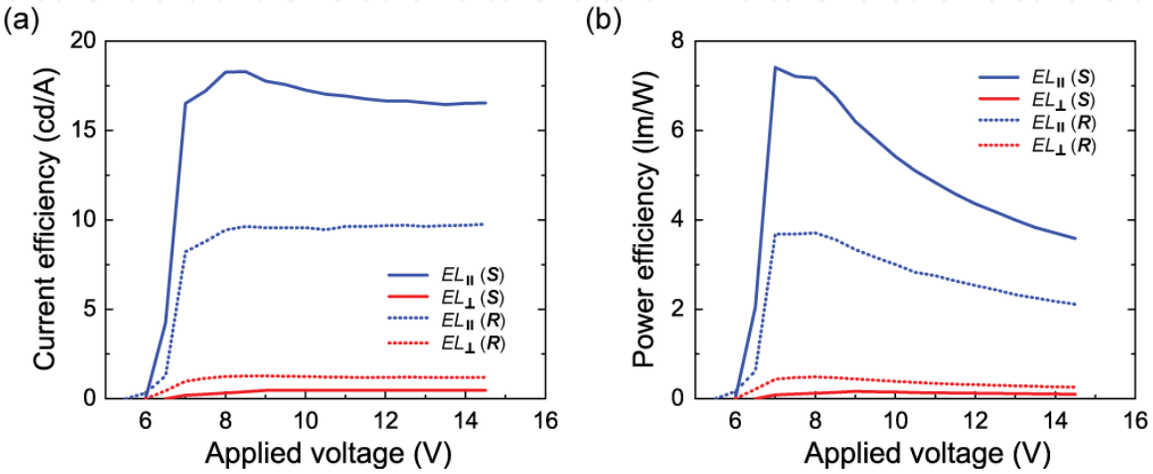

Figure 15. (a) Current efficiency-voltage and (d) power efficiency-voltage characteristics of Reference (*R*, dotted curves) and Sample (*S*, solid curves) WOLEDs.

Next, we have estimated the relationship between polarization ratio and luminance *PR-L* for the polarized WOLED *S*, thereby presenting quantitative results for the polarized emissions. Figure 16(a) shows that the highly polarized characteristics of the polarized WOLED *S* give a high average value of *PR* ($EL_{||}$: $EL\perp$) of at least ~35:1 over the whole range of brightness. It should be noted that this value of *PR* is significantly higher than that of device *R* (8.21:1). In order to understand the characteristics of the polarized EL, we have measured the polarized emission spectra for $EL_{||}$ (blue curves) and $EL\perp$ (red curves) for the device *S* under an applied voltage of 10 V (Figure 16(b)). It may be noted that the spectral shape of the $EL_{||}$ for device *S* is very similar to that for device *R*. The observed color rendering index (CRI) of $EL_{||}$ for device *S* is about 80.0, and the CIE XYZ color space is (0.285, 0.363, 0.353), with a correlated color temperature (CCT) of about 7,600 K. These characteristics are also similar to those of $EL_{||}$ from device *R*, which has a CRI of about 74.0, CIE XYZ color space of (0.275, 0.342, 0.383), and CCT of about 8,500 K. At the same time Figure 16(b) also shows that the polarized EL emission spectrum depends very much on the polarization state and that device *S* produces highly polarized EL emission over the whole spectrum. For the device *S*, the highest value of *PR* calculated from the integrated intensities of the parallel and perpendicularly polarized EL spectra is approximately 35:1, which is significantly higher than that of the white-light emitting devices that use uniaxially oriented materials [17]. These results prove that our polarized WOLED (*S*), which incorporates an achromatic QWP film with a GBO reflective polarizer, outperforms all other similar devices.

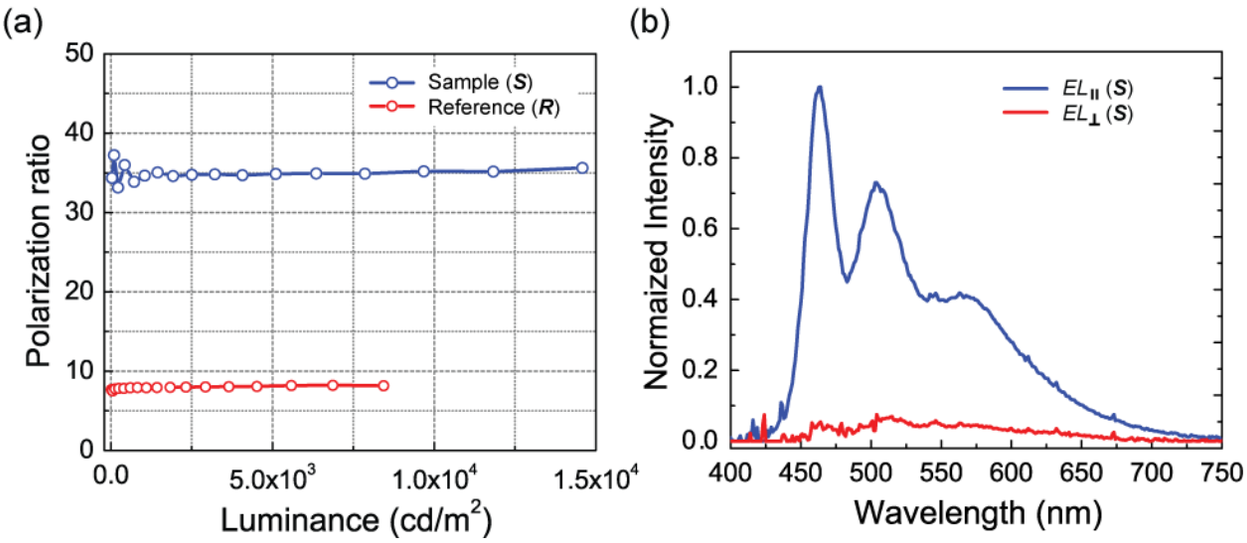

Figure 16. (a) Polarization ratios of the polarized WOLEDs against luminance. (b) Polarized EL spectra of $EL_{||}$ (blue curve) and $EL_{\perp}$ (red curve) of the sample WOLED *S* at 10 V.

Finally, we have shown in Fig. 17 the photographs of the performance of WOLEDs (1 mm × 1 mm) operating under the same bias voltage of 8 V for polarizations along the passing (upper) and blocking (lower) axes of the GBO reflective polarizer. Fig. 17 shows clearly that under a rotating linear dichroic polarizer, the EL emission from device *S* is fairly brighter and more highly polarized along the passing axis of the GBO polarizer, compared to that of device *R*.

2.3.3. Summary

In summary, we have described the fabrication and investigation of the properties of a polarized WOLED using a combination of an achromatic QWP and a GBO reflective polarizer. By applying the achromatic QWP and the GBO polarizer to the WOLED, polarized EL brightnesses in excess of ca. 14,600 cd/m² can be obtained from the polarized WOLED, together with high peak efficiencies of more than 18 cd/A (7.4 lm/W), which are almost double of those obtained from the polarized WOLED with only the GBO polarizer. We have also found that a high polarization ratio of ca. 35:1 is possible over the whole range of brightness of the emissions. Although the *PR* value of the polarized WOLED is slightly lower than that of polarized narrow band (green) OLED in section 2.2, it may be noted that only the polarized WOLED can provide a polarized light source for a wide range of wavelengths from the blue through to the green and red color regions.

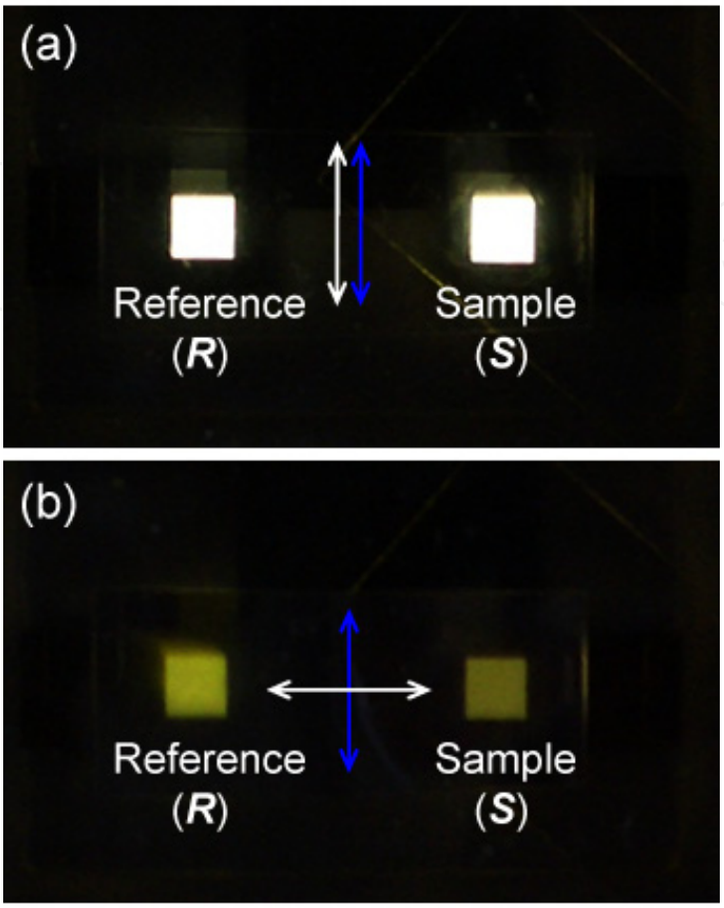

Figure 17. Photographs of the brightness obtained from the reference (*R*, left) and sample (*S*, right) WOLEDs (at 8 V) for $EL_{||}$ (a) and $EL_{\perp}$ (b) under a rotating linear dichroic polarizer film. The white and blue arrows represent the transmission axes of the linear dichroic polarizer and the GBO polarizer, respectively. The active areas of the polarized WOLEDs were 1 mm × 1 mm. (It may be noted that the device *R* appears to be brighter than device *S* in Fig (b) because device *S* is more highly polarized along the passing axis of the GBO polarizer, compared to that of device *R*.)

3. Conclusions

We have fabricated flexible, polarized, and luminous OLEDs using a flexible GBO reflecting polarizer substrate. We have also described the fabrication and investigation of a polarized and luminous OLED and WOLED using a combination of a QWP retardation film and a GBO reflective polarizer. Polarized EL brightnesses of over 10,000 cd/m² can be produced from the polarized OLED, with high peak efficiencies in excess of 10 cd/A, which are almost double those obtained from the polarized WOLED with only the GBO polarizer. The polarization direction of the EL light emitted from the polarized OLED corresponds to the passing axis of the GBO polarizer used. Furthermore, we have also shown that a high polarization ratio of greater than 35~40 is possible over the whole emission brightness

range. These results show that using the (achromatic) QWP film and the GBO reflective polarizer one can develop bright (W)OLEDs with highly polarized luminescence emissions. It is also noted that the polarization ratio of the polarized WOLED can be further improved by introducing a high quality achromatic QWP film for a wide range of wavelengths including red, green, and blue light. By combining the devices presented here with the luminous EL layers reported elsewhere [35], it may be possible to develop highly efficient polarized OLEDs with a wide range of optical applications. For example, the device structure used in this study can be applied to the design of special light-emitting devices, such as polarized backlights for LC displays. Such devices can also be used for the development of a new class of polarized OLEDs such as polarized surface emitting devices for 3-D displays and/or the polarized light sources of optical waveguide devices.

Author details

Byoungchoo Park
Department of Electrophysics, Kwangwoon University, Seoul, Korea

Acknowledgement

This work was supported by the National Research Foundation of Korea(NRF) grant funded by the Ministry of Education, Science and Technology, Republic of Korea (20120003831 and 2012015654). This research was also supported by the Converging Research Center Program through the Ministry of Education, Science and Technology (2012K001303) and the leading industry of NEW-IT and equipments of the Chungcheong Leading Industry Office of the Korean Ministry of Knowledge Economy (A002200104).

4. References

[1] C. W. Tang, S. A. Van Slyke, Organic electroluminescent diodes. Applied Physics Letters 51, 913 (1987).

[2] R. H. Friend, R. W. Gymer, A. B. Holmes, J. H. Burroughes, R. N. Marks, C. Taliani, D. D. C. Bradly, D. A. Dos Santos, J. L. Bredas, M. Logdlund, W. R. Salaneck, Electroluminescence in conjugated polymers. Nature (London) 397, 121 (1999).

[3] M. A. Baldo, S. Lamansky, P. E. Burrows, M. E. Thompson, S. R. Forrest, Very high-efficiency green organic light-emitting devices based on electrophosphorescence. Applied Physics Letters 75, 4 (1999).

[4] M. Ikai, S. Tokito, Y. Sakamoto, T. Suzuki, Y. Taga, Highly efficient phosphorescence from organic light-emitting devices with an exciton-block layer. Applied Physics Letters 79, 156 (2001).

[5] C. Adachi, M. E. Thompson, S. R. Forrest, Architectures for efficient electrophosphorescent organic light-emitting devices. IEEE Journal of Selected Topics in Quantum Electronics 8, 372 (2002).

[6] V. Cimrova, M. Remmers, D. Neher, G. Wegner, Polarized light emission from LEDs prepared by the Langmuir-Blodgett technique. Advanced Materials 8, 146 (1996).
[7] M. Jandke, P. Strohriegl, J. Gmeiner, W. Brutting, M. Schwoerer, Polarized electroluminescence from rubbing-aligned poly(p-phenylenevinylene). Advanced Materials 11, 1518 (1999).
[8] D. X. Zhu, H. Y. Zhen, H. Ye, X. Liu, Highly polarized white-light emission from a single copolymer based on fluorine. Applied Physics Letters 93, 163309 (2008).
[9] P. Dyreklev, M. Berggren, O. Inganas, M. R. Andersson, O. Wennerstrom, T. Hjertberg, Polarized electroluminescence from an oriented substituted polythiophene in a light emitting diode. Advanced Materials 7, 43 (1995).
[10] C. C. Wu, P. Y. Tsay, H. Y. Cheng, S. J. Bai, Polarized luminescence and absorption of highly oriented, fully conjugated, heterocyclic aromatic rigid-rod polymer poly-p-phenylenebenzobisoxazole. Journal of Applied Physics 95, 417 (2004).
[11] M. Grell, D. D. C. Bradley, Polarized luminescence from oriented molecular materials. Advanced Materials 11, 895 (1999).
[12] K. Sakamoto, K. Miki, M. Misaki, K. Sakaguchi, M. Chikamatsu, R. Azumi, Very thin photoalignment films for liquid crystalline conjugated polymers: Application to polarized light-emitting diodes. Applied Physics Letters 91, 183509 (2007).
[13] K. Pichler, R. H. Friend, P. L. Burn, A. B. Holmes, Chain alignment in poly(p-phenylene vinylene) on oriented substrates. Synthetic Metals 55, 454 (1993).
[14] M. Era, T. Tsutsui, S. Saito, Polarized electroluminescence from oriented p-sexiphenyl vacuum-deposited film. Applied Physics Letters 67, 2436 (1995).
[15] M. Misaki, Y. Ueda, S. Nagamatsu, M. Chikamatsu, Y. Yoshida, N. Tanigaki, K. Yase, Highly polarized polymer light-emitting diodes utilizing friction-transferred poly(9, 9-dioctylfluorene) thin films. Applied Physics Letters 87, 243503 (2005).
[16] M. Misaki, M. Chikamatsu, Y. Yoshida, R. Azumi, N. Tanigaki, K. Yase, S. Nagamatsu, Y. Ueda, Highly efficient polarized polymer light-emitting diodes utilizing oriented films of β-phase poly(9, 9-dioctylfluorene). Applied Physics Letters 93, 023304 (2008).
[17] A. Liedtke, M. O' Neill, A. Wertmoller, S. P. Kitney, S. M. Kelly, White-Light OLEDs Using Liquid Crystal Polymer Networks. Chemistry of Materials 20, 3579 (2008).
[18] I. H. H. Zabel, D. Stroud, Photonic band structures of optically anisotropic periodic arrays. Physical Review B 48, 5004(1993).
[19] Z. Y. Li, J. Wang, B. Y. Gu, Creation of partial band gaps in anisotropic photonic-band-gap structures. Physical Review B 58, 3721 (1998).
[20] G. Alagappan, X. W. Sun, P. Shum, M. B. Yu, M. T. Doan, One-dimensional anisotropic photonic crystal with a tunable bandgap. Journal of the Optical Society of America B 23, 159 (2006).

[21] J. P. Dowling, M. Scalora, M. J. Bloemer, C. M. Bowden, The photonic band edge laser: A new approach to gain enhancement. Journal of Applied Physics 75, 1896 (1994).

[22] T. Matsui, R. Ozaki, K. Funamoto, M. Ozaki, K. Yoshino, Flexible mirrorless laser based on a free-standing film of photopolymerized cholesteric liquid crystal. Applied Physics Letters 81, 3741 (2002).

[23] J. Hwang, M. H. Song, B. Park, S. Nishimura, T. Toyooka, J. W. Wu, Y. Takanishi, K. Ishikawa, H. Takezoe, Electro-tunable optical diode based on photonic bandgap liquid-crystal heterojunctions. Nature Materials 4, 383 (2005).

[24] M. H. Song, B. Park, S. Nishimura, T. Toyooka, I. J. Chung, Y. Takanishi, K. Ishikawa, H. Takezoe, Electrotunable Non-reciprocal Laser Emission from a Liquid-Crystal Photonic Device. Advanced Functional Materials 16, 1793 (2006).

[25] H. Zhang, H. You, W. Wang, J. Shi, S. Guo, M. Liu, D. Ma, Organic white-light-emitting devices based on a multimode resonant microcavity. Semiconductor Science and Technology 21, 1094 (2006).

[26] A. Dodabalapur, L. J. Rothberg, T. M. Miller, Color variation with electroluminescent organic semiconductors in multimode resonant cavities. Applied Physics Letters 65, 2308 (1994).

[27] J. Lim, S. S. Oh, D. Y. Kim, S. H. Cho, I. T. Kim, S. H. Han, H. Takezoe, E. H. Choi, G. S. Cho, Y. H. Seo, S. O. Kang, B. Park, Enhanced out-coupling factor of microcavity organic light-emitting devices with irregular microlens array. Optics Express 14, 6564 (2006).

[28] M. F. Weber, C. A. Stover, L. R. Glbert, T. J. Nevitt, A. J. Ouderkirk, Giant birefringent optics in multilayer polymer mirror. Science 287, 2451 (2000).

[29] B. Park, C. H. Park, M. Kim, M.-Y. Han, Polarized organic light-emitting device on a flexible giant birefringent optical reflecting polarizer substrate. Optics Express 17, 10136 (2009).

[30] B. Park, Y. H. Huh, H. G. Jeon, Polarized electroluminescence from organic light-emitting devices using photon recycling. Optics Express 18, 19824 (2010).

[31] B. Park, Y. H. Huh, S. H. Lee, Y. B. Kim, Linearly-polarized White-light-emitting OLEDs Using Photon Recycling. Journal of the Korean Physical Society 59, 341 (2011).

[32] B. Park, M. Y. Han, S. S. Oh, Solution processable ionic p-i-n phosphorescent organic light-emitting diodes. Applied Physics Letters 93, 093302 (2008).

[33] J. M. Bendickson, J. P. Dowling, M. Scalora, Analytic expressions for the electromagnetic mode density in finite, one-dimensional, photonic band-gap structures. Physical Review E 53, 4107 (1996).

[34] S. V. Belayev, M. Schadt, M. I. Barnik, J. Funfschilling, N. V. Malimoneko, K. Schmitt, Large Aperture Polarized Light Source and Novel Liquid Crystal Display Operating Modes. Japanese Journal of Applied Physics 29, L634 (1990).

[35] Y.-S. Tyan, Y. Q. Rao, X. F. Ren, R. Kesel, T. R. Cushman, W. J. Begley, N. Bhandari, Tandem Hybrid White OLED Devices with Improved Light Extraction. SID Symposium Digest of Technical Papers 40, 895 (2009).

IntechOpen